Lineaments Analysis of Tabnak Field Using LANDSAT Images

Bahram Habibnia[1,*], Seyyed Mahmood Ghodosi Nejad[1], Samira Emadi[1]

1- Abadan Faculty of Petroleum Engineering, Petroleum University of Technology, Abadan, Iran.

* Corresponding Author: B.habibnia@gmail.com

Abstract

Geological studies are basic form of operations for the exploration and development of oil and gas fields. Preparation of topographical and geological maps and drawing cross section from these maps forms part of these operations. Existing lineaments in the study area are important, and should be considered in drawing the geological sections. The evaluation of wells stability is one of the important issues in engineering geology, because the instability of walls means the acceptance of unknown risks. The existing lineaments in the area can have an important role in the stability or instability of the walls of wells. The purpose of this study is to investigate surface lineaments arrangements. To achieve this goal, Landsat satellite images were used. Images were processed using different techniques and lineaments map was provided. In the next stage, artificial lineaments were removed from lineaments map and remaining lineaments largely reflected existing fractures in the region. In order to study more precise lineaments, field studies were conducted at 3 stations and dip and strike of fractures were measured at each station and rosette plot, contour plot, scatter plot and pole plot were plotted for each station. The results of this study show that the density of lineaments in different parts of the field is not the same, but in the northwestern part of the field, lineaments density is higher than the other parts. Lineaments extend in different directions, but the extension of lineaments in NE-SW direction is dominant.

Keywords: Lineaments, Image processing, Fracture, Satellite images, Arrangement.

1– Introduction

Tabnak gas field is an exposed anticline located in the mountainous area of the sub coastal Fars province in southern Iran. In relation to the top of the Dehram group, Tabnak is a deeper horizon compared with the other anticlines of Assaluyeh range. The northeastern flank of the structure is steep dipping. From exposed outcrops to the target, formations are consisted of mainly limestone and dolomite and secondly shale with inter bedded chert and yellow iron. Laffanh and Kazhidumi formations primarily consist of shale. The formations below Gadvan are dominated by limestone and dolomite with beds of blackish gray, grayish-green and massive shale. Some limestone is much more argillaceous (Guang *et al*., 2006). The topographic and geological map and location of Tabnak field are shown in Figures 1 and 2. Lineaments are natural simple or composite-pattern linear or curvilinear features discernible on the Earth's surface. In the geologic sense, these features may depict crustal structure or may represent a zone of structural weakness. These originate mainly from strains that arise from stress concentrations around flaws,↓ heterogeneities, and physical discontinuities, largely reflected in the form of faults, fractures and joint sets. They form in response to lithostatic, tectonic, and thermal stresses and high fluid pressures. They occur at a variety of scales, from microscopic to continental.

Fractures are important in engineering, geotechnical, and hydrogeological practice because they provide pathways for fluid flow (Masoud and Koike, 2006). Lineament mapping and analysis from remote sensing data is an important approach for regional structural and tectonic studies (Solomon and Ghebreab, 2006).

Figure 1) The topographic map and location of Tabnak field

Lineaments interpretation is conducted based on the information extracted from air-photograph. Then satellite images were more frequently used for this purpose. However, in Malaysia the Landsat images used in geological mapping and lineaments interpretation are produced from non-digitally enhanced data (Foo, 1976; Sudrajat, 1978; Raj, 1982; Tjia and Zaiton, 1985; Almashoor and Tijia, 1987; Tijia, 1989; Lai, 1990). The advantages of using digitally processed satellite data are very well known and they have been shown by several researchers (Rowan et. al., 1974; Siegev land Abram, 1976; Condit and Chaves, 1979; Blodged and Brown, 1982; Rothery, 1985). For this reason, in the more recent work, the use of enhanced digitally processed satellite data was becoming more popular and this type of data was frequently used in either geological mapping as well as in lineament interpretation and mapping (Juhari, 1990, 1991 and 1996; nor Bakri, 1993; Azlikamil *et al*., 1996; Noraini *et al*., 1996). The purpose of this study is to investigate surface lineaments arrangements. To achieve this goal, Landsat satellite images were used. Images were processed using different techniques and lineaments map was provided. In the next stage, artificial lineaments were removed from lineaments map and remaining lineaments largely reflected existing fractures in the region. In order to study more precise lineaments, field studies were conducted at 3 stations and dip and strike of fractures were measured at each station and rosette plot, contour plot, scatter plot and pole plot were plotted for each station. The orientation of an induced wellbore fracture is a major factor in planning and developing an oil-recovery operation. Lineament patterns determined from surface surveys and/or aerial photographs can be correlated with subsurface fracture orientation data and used to predict the bearing of hydraulically induced wellbore fractures (William *et al*., 1968).

If we want to estimate a horizontal well's production potential before it is drilled, stochastic simulation techniques have to be used to simulate the fracture system in the subsurface. The probability distribution functions obtained from the analyses of surface lineaments and fractures provide some basic probability models for simulating subsurface fracture orientation, length, and spacing. The key to the success of a horizontal well drilling program in producing a naturally fractured reservoir is to obtain a realistic description of the subsurface natural fractures. Surface and subsurface fractures in many parts of the world are very consistent in orientation. At least some sets of surface fractures mapped from outcrop studies can be, to a certain degree, extrapolated to subsurface formations (Guo *et al*., 1996).

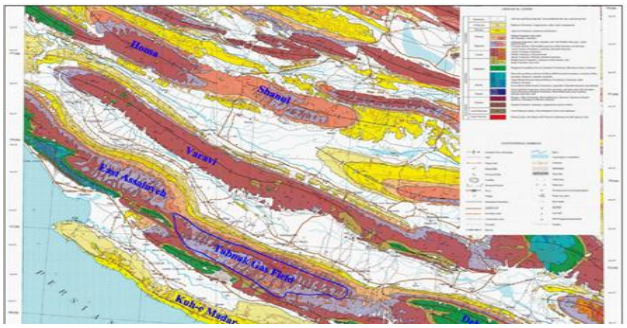

Figure 2) Geological map and Location of Tabnak field

2– Methodology

2.1- Preprocessing

Before the main processing, some corrections must be applied to satellite images. Usually remote sensing data that are received by remote sensing systems are influenced by two major errors (radiometric and geometric errors). In radiometric error, the content of the recorded information by remote sensing systems is affected and this causes the numeric value for each pixel (Digital Number or DN Value) and the value of true reflection of the corresponding phenomena to be inconsistent. Geometric error changes the geometry of picture, including size and shape. This error causes the size and shape of pixels in the images to be contrary to the real size and shape of phenomenon on the earth. Raw images taken by satellites are in the pixel coordinate system that must be connected to the global coordinate system. The image on which preprocessing is performed is radiometrically and geometrically close to reality as much as possible.

2.2- False color image preparation

The ETM^+ satellite images which are used in this study are gray (non-tinted) and are not clear. So at this stage it is necessary to create a false color image. This image is a combination of three different bands which are associated with each of three colors, i.e. red, green and blue (RGB). It is much easier to distinguish and identify the structural features in a color image than a gray image.

2.3- Histogram modification

Histogram is the graphical representation of brightness values of pixels versus number of occurrences in the whole image. Horizontal axis of histogram is the amount of light of each pixel and the vertical axis represents the number of pixels that have the same amount of light. Radiometric quality of image can be evaluated by its histogram. When the histogram of an image is extended in total radiometric measuring range, the image has a good radiometric quality. So at this stage, if the image has a poor radiometric quality, or in other words, the histogram distribution is not appropriate, histogram modification should be applied to the histogram of the image, so that the histogram of the image will fit within a good radiometric range.

2.4- Geometric enhancement

At this stage, the image quality in terms of spatial (geometric) is improved, and a new value for each pixel is calculated. This new value is obtained from the brightness values of neighborhood (neighboring or adjacent) pixels. For this purpose, filtering or neighborhood operator is used. Where there are lineaments and fractures, severe and sudden changes of pixel values in a small region of the image occur, so it is better to use high pass filters. These filters try to remove low frequency and keep high frequency. A high frequency part of the image includes sudden changes of grade lighting in a short distance. The matrix is moved on the original image and the weight of each pixel in the corresponding brightness values in the original image is multiplied and the sum of this multiplication is placed as new brightness value in the central pixel of window. Movement of matrix continues in the whole image and this operation is carried out pixel by pixel. The high pass filters cause high-frequency area, such as lineaments, to be more specific than elsewhere and thus the resulting image has more detail and is more specific.

2.5- Removal of artificial lineaments

Up to this point, by improving of the quality of images and applying of the appropriate filter, lineaments are enhanced and extracted. But some of these lineaments are synthetic and correspond to the linear features such as roads, railways, waterways and rivers. In the geological studies and exploration of oil, the

study of fractures and faults is important; therefore, the artificial lineaments are deleted from the lineaments map. For this purpose, topographic and geologic maps of the study area are used (Figs. 1 and 2) and lineaments that correspond to roads, waterways, railways, etc. are removed. The remaining lineaments correspond to fractures and faults in the study area.

3– Results and discussion

3.1- Input data

For investigation of lineaments, ETM^+ images which were acquired by the Landsat7 satellite have been used. These images consist of a range about 185×170 km^2 and their cell size is 30 meters. Visible bands of these images have wavelengths as shown in Table 1.

Landsat 7 satellite was launched in 1999 and the resulting images have 7 spectral bands and their nominal revisit interval is 8 days. These images are easy to access and low in prices so they are more common. Bands#1, 3 and 7 were used for this study. These bands have 30-meters spatial resolution and 8-bits radiometric resolution. The wavelengths of other bands are shown in Table 2.

Table 1) Images wavelengths.

Blue (µm)	Green (µm)	Red (µm)
0.45-0.515	0.525-0.605	0.63-0.69

The spatial resolution of all bands except band 6 is 30 meters. Resolution of band 6 is 60 meters. Due to the geographical location of the Tabnak field, ETM^+ images of row # 41 and path # 162 were used in this study.

Table 2) Wavelength of other bands.

Band#4(µm)	Band#5(µm)	Band#6(µm)	Band#7(µm)
0.75-0.9	1.55-1.75	10.4-12.5	2.08-2.35

3.2- False color preparation

As mentioned, each satellite image is composed of a number of pixels and each pixel has a digital number (DN) that represents the brightness of pixel. Table 3 is a schematic diagram of some pixels with their DN. Also, Table 3b shows statistical data of the digital numbers of images for each band separately. The first step in image processing is corrections performance images used in this study is level 1T and geometric and radiometric corrections have been applied on them.

Table 3) Schematic of some pixels with their DN.

170	238	85	255	221	0
68	136	17	170	119	68
221	0	238	136	0	255
119	255	85	170	136	238
238	17	221	68	119	255
85	170	119	221	17	136

Each band is black-white by itself and structures are not visible on it excellently. So at this stage, bands#1, 3 and 7 are combined to create a color image. The Table 4 shows the correlation matrix between different bands.

Table 3b) Statistical data of the DN of images for each band.

Index	band#1	band#3	band#7
Minimum	0.000	0.000	0.000
Maximum	212.000	245.000	255.000
Mean	43.169	43.000	36.350
Median	44.000	18.000	8.000
Std. Dev.	33.888	46.174	43.664
Std. Dev. (n-1)	33.888	46.174	43.664
Corr. Eigenval.	1.000	1.000	1.000
Corr. Eigenval.	1148.409	2132.013	1906.571

Table 4) Correlation matrix between different bands.

Correlation Matrix	Band #1	Band #3	Band #7
Band #1	1	0.974	0.941
Band #3	0.974	1	0.972
Band # 7	0.941	0.972	1

3.3- Histogram modification

The histogram of image in the study area does not include whole (0-255) interval and DNs of pixels in each band have been limited to a smaller range. These ranges are between 40 and 134 for band#1, 15 and 187 for band#3, 3 and 165 for band#7. Therefore, histogram modification was performed to improve the image quality and more marking of lineaments. In this way, the dark points of image will be darker and the bright points of image will be brighter and image quality increases. The histograms of bands#1, 3 and 7 before and after histogram modification are shown in the Figures 3 to 8. The Figures 9 and 10 show the satellite image of Tabnak gas field before and after histogram modification.

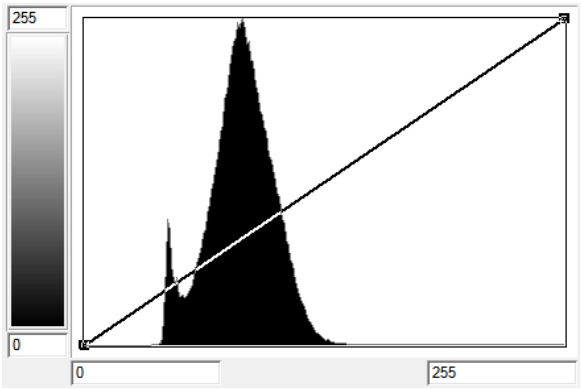

Figure 3) Histogram of band#1 before histogram modification.

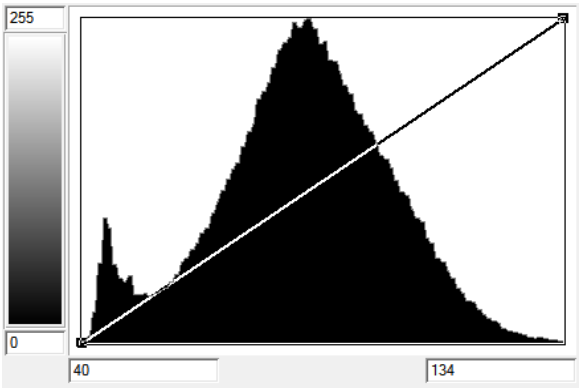

Figure 4) Histogram of band#1 after histogram modification.

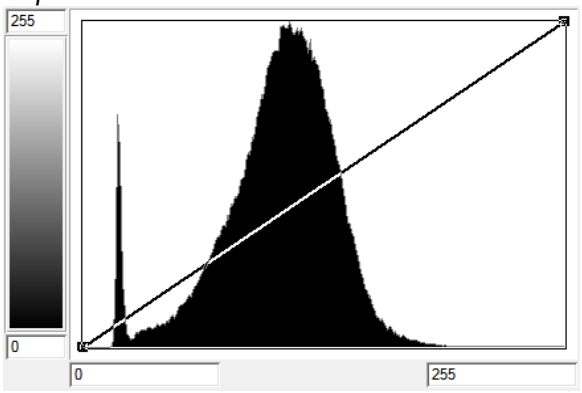

Figure 5) Histogram of band#3 before histogram modification.

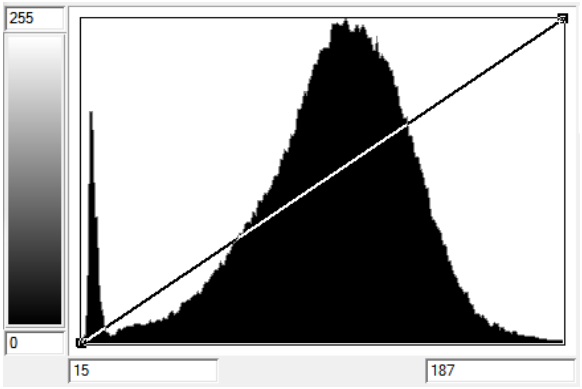

Figure 6) Histogram of band#3 after histogram modification.

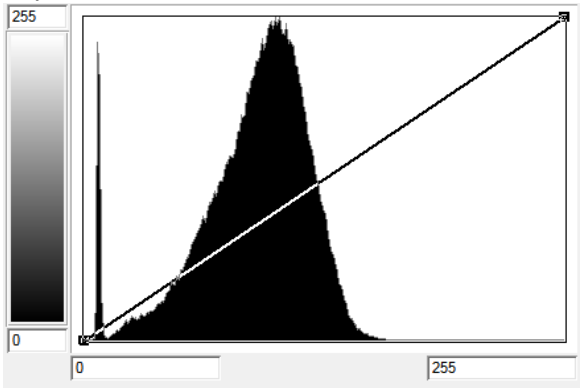

Figure 7) Histogram of band#7 before histogram modification.

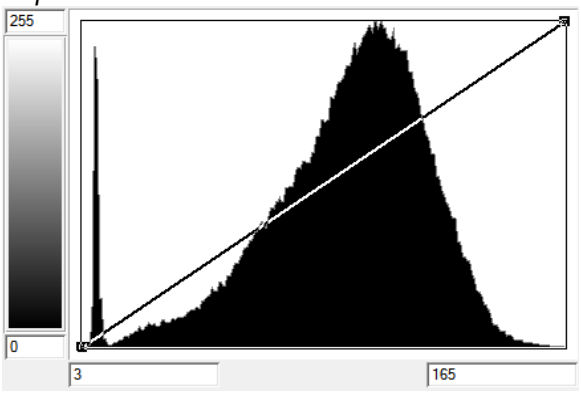

Figure 8) Histogram of band#7 after histogram modification.

3.4- Geometric enhancement

After histogram modification, for detection and extraction of lineaments in the study area a filter was used. This filter is a matrix which has 25 elements. Figure 11 depicts the matrix of filter. This filter moves on the satellite image and

convolution is done between the filter and the image. Figure 12 shows satellite image after applying the filter. As can be seen in the figure, lineaments are more apparent after filtering.

3.5- Removal of artificial lineaments

For the investigation of strike of lineaments, the field was divided into 3 sections: northwest, center and south-east. Then rosette diagram was plotted for each section. The rosette diagrams are radial histogram of strike density. They convey less information than a full stereo net since one dimension is removed from the diagram. From a visualization point of view and for simple conveying structural data, rosettes may be more appropriate than other diagrams.

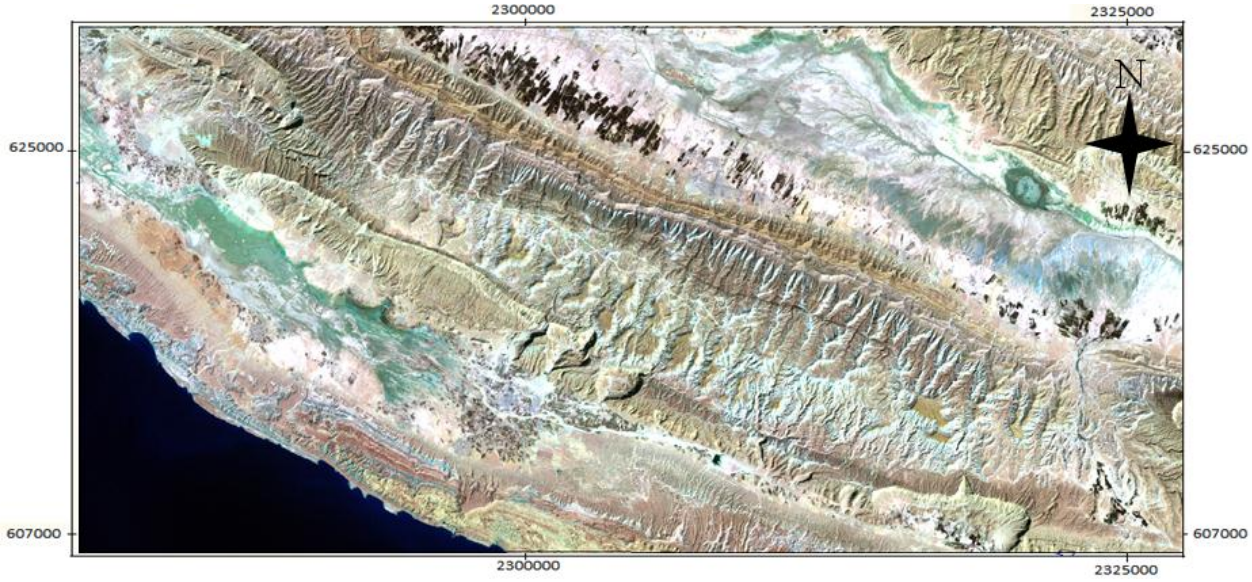

Figure 9) Satellite image of field before histogram modification.

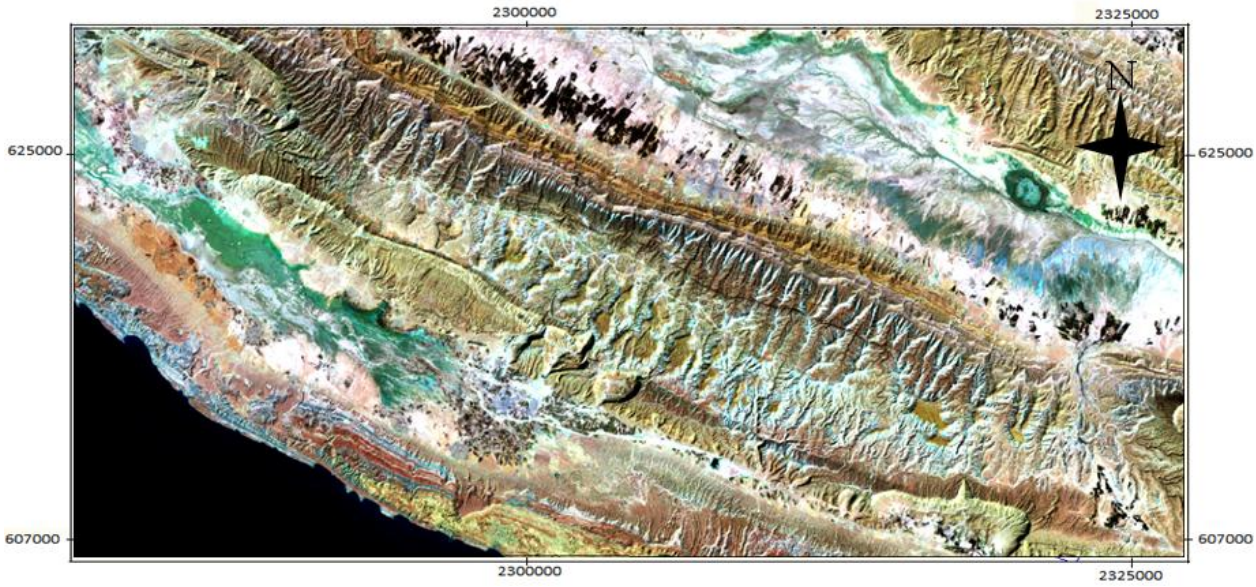

Figure 10) Satellite image of field after histogram modification.

	1	2	3	4	5
1	-1	-1	-1	-1	-1
2	-1	-1	-1	-1	-1
3	-1	-1	49	-1	-1
4	-1	-1	-1	-1	-1
5	-1	-1	-1	-1	-1

Figure 11) Matrix of filter.

After the processing, 847 lineaments were extracted in the region. As can be seen in the Figure 13, the density of lineaments in north-western part of the field is higher than other parts.

Northwest field:

The Figure 14 depicts rosette plot of lineaments in the northwestern part of the field. As the rosette plot above shows in this part of the field, lineaments have strikes in different directions, but they are dominantly oriented in the NE-SW direction. Three lineament sets are dominant in this part and they have strikes in N20ºE to N50ºE directions.

Southeast field:

The rosette plot of lineaments in the southeastern part of the field is shown in Figure 15. The rosette diagram shows in this part of the field, lineaments have strikes in different directions. The orientation of lineaments is dominantly NE-SW. Two lineament sets are dominant in this part and they have strikes in N80º-90ºW and N0º-10ºE directions.

Center of the field:

The Figure 16 shows rosette plot of lineaments in the central part of the field. The rosette plot shows lineaments have strikes in different directions. The dominant orientation of lineaments is ENE-WSW in this part of the field. Three lineament sets are dominant and they have strikes in N80º-90ºW, N40º-50ºE and N0º-10ºE directions.

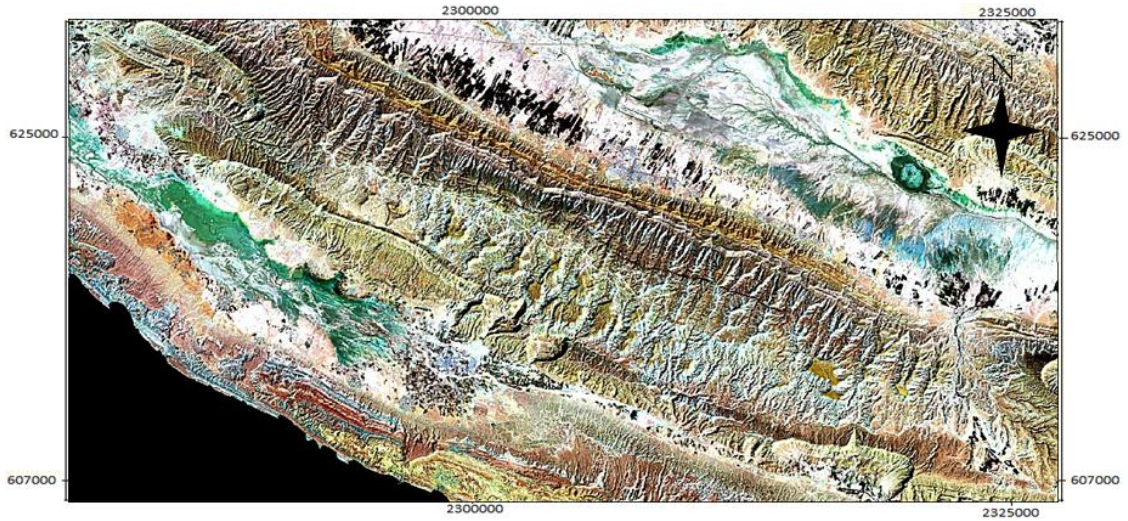

Figure 12) Satellite image after applying the filter.

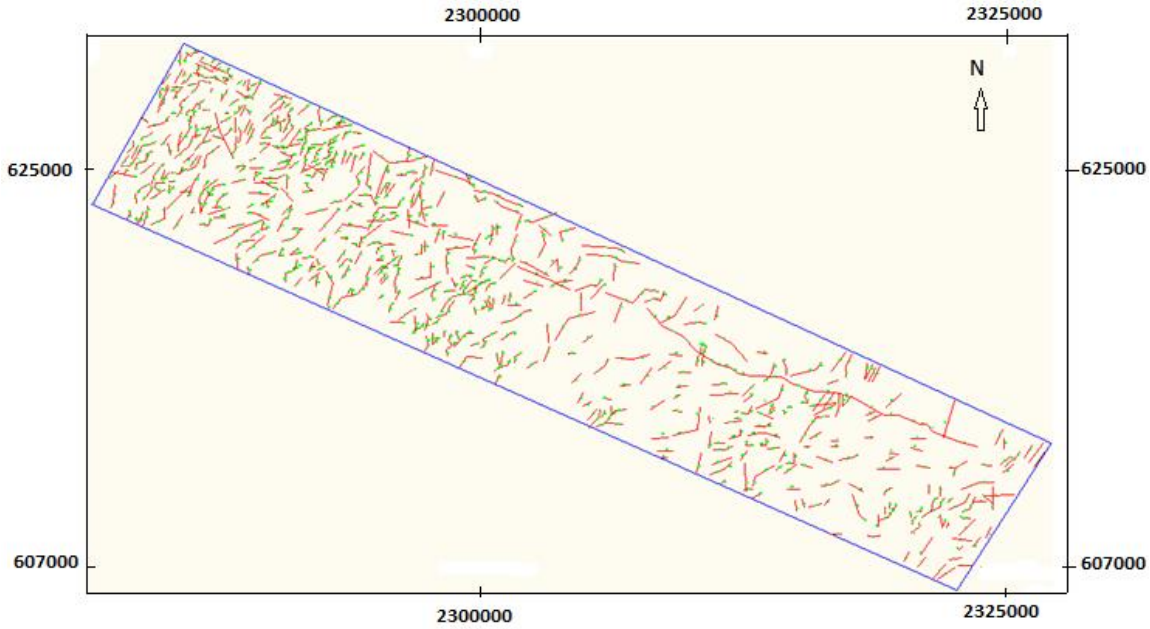

Figure 13) Lineaments Map.

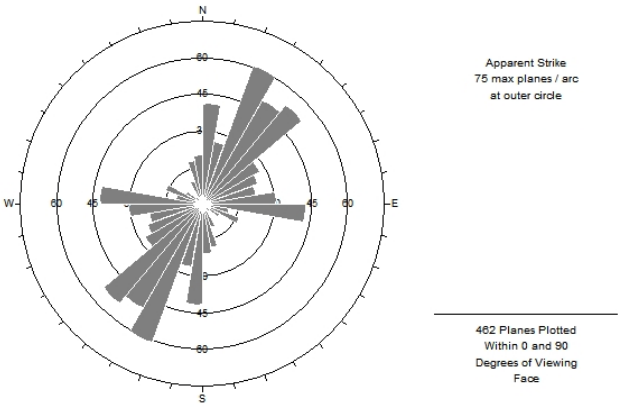

Figure 14) Rosette plot for strike of lineaments in the NW (North-West) field.

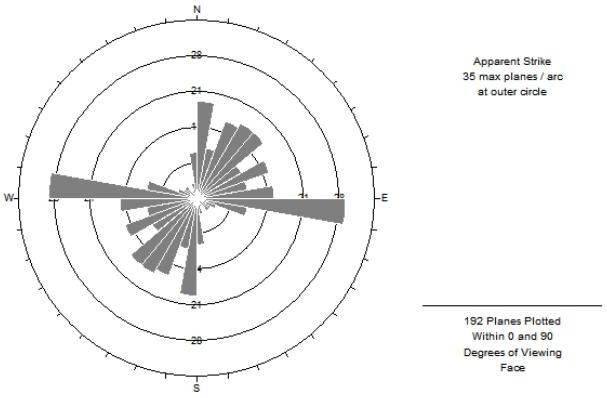

Figure 15) Rosette plot for strike of lineaments in the SE (South-East) field.

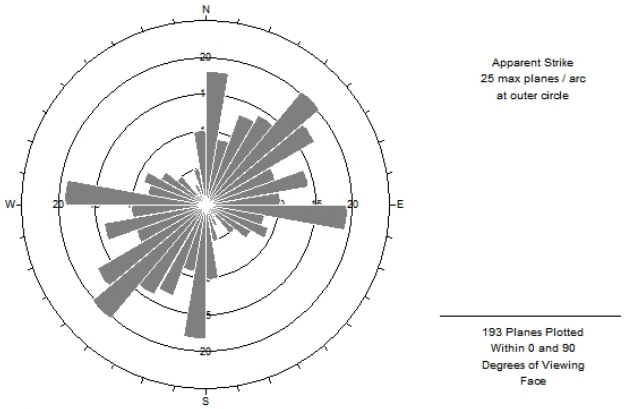

Figure 16) Rosette Diagram for strike of lineaments in central part of the field.

Total of the field:

Figure 17 depicts rosette plot of lineaments in total of the field. The rosette plot shows lineaments have strikes in different directions. The dominant orientation of lineaments is NE-SW. Three lineament sets are dominant and they have strikes in N80º-90º W, N40º-50ºE and N20º-30ºE directions.

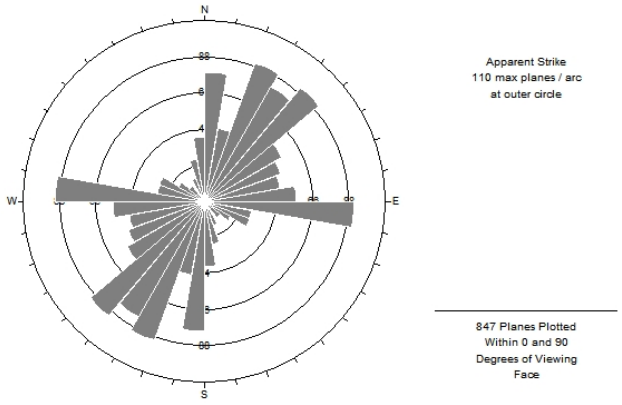

Figure 17) Rosette plot for strike of lineaments in total of the field.

Extracted lineaments are not just related to fractures and faults, but some are related to water ways, roads and etc. Since only the lineaments that are related to fractures and faults are important and so other lineaments should be removed from lineament map. For this purpose, topographic and geologic maps of the study area are used to remove lineaments that related to roads, water ways and etc. Figure 18 shows the lineaments map after removal of artificial lineaments. As can be seen a significant number of lineaments are artificial and have been removed.

3.6- Field Study

Finally, to verify the extracted lineaments orientation, field studies were conducted and strike and dip of the lineaments were measured at three stations by compass. Figure 19 shows the location of stations.

3.6.1- First station

This station has coordinate E: 2283150 and N: 625920 that N indicates the vertical axis and E indicates the horizontal axis and numbers are in the Lambert coordinates. Lithology at this station is limestone and Asmari-Jahrum formations are exposed. The next table shows strike and dip of measured lineaments at this station. Figures 20 shows rosette plot of lineaments at first station. The rosette plot

showing two main strikes and they are in N20º-30ºE and N40º-50ºE directions.

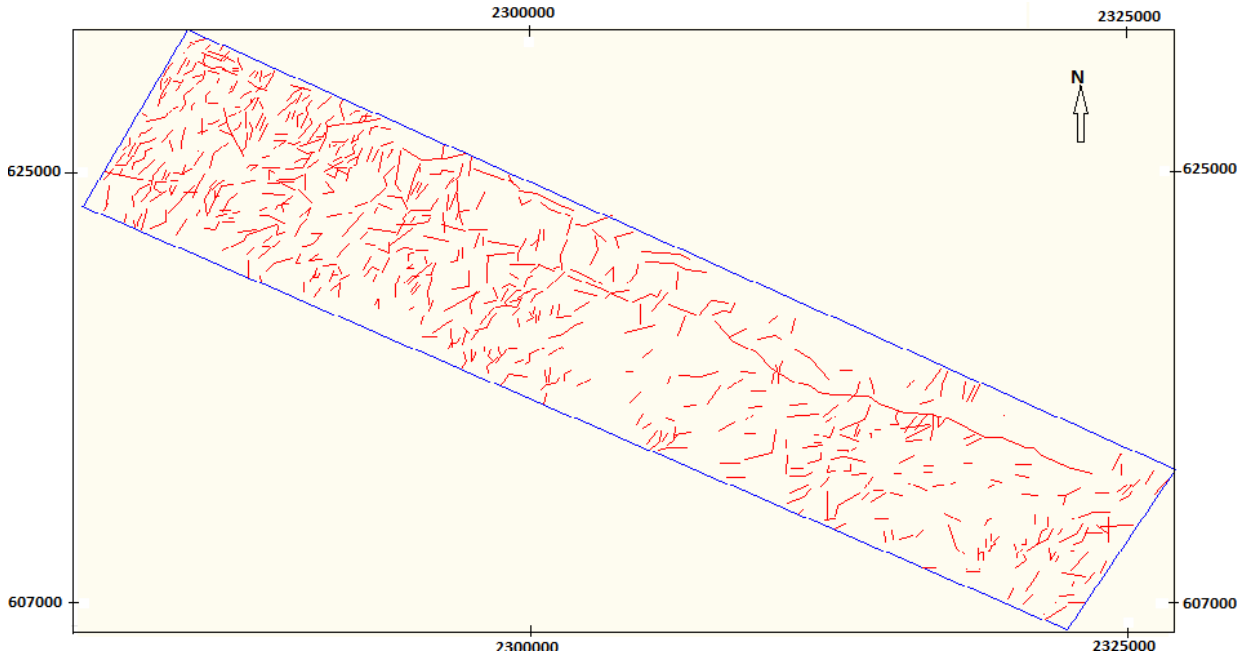

Figure 18 Lineaments map after removal of artificial lineaments.

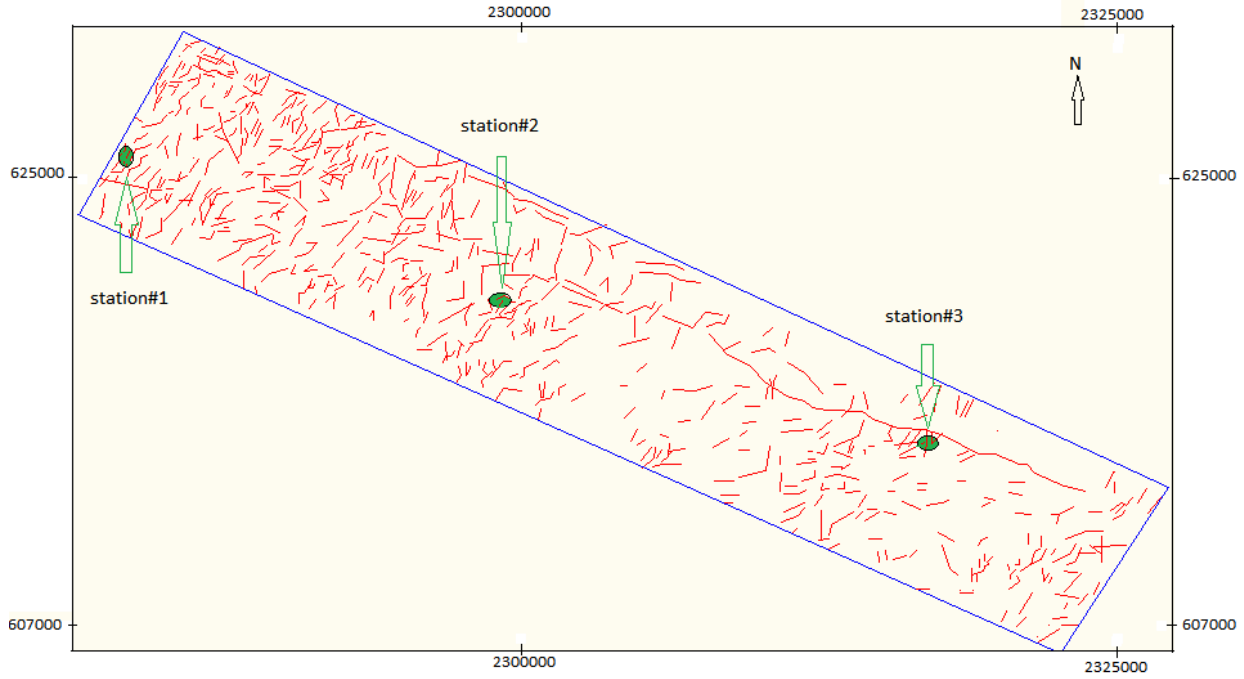

Figure 19 Location of stations.

3.6.2- Scond station

This station has coordinate E (Easting): 2298830 and N (Northing): 620330 and numbers are in the Lambert coordinates. Lithology at this station is dolomitic limestone and Asmari-Jahrum formations are exposed. Figure 21 shows rosette plot of lineaments at second station. The rosette plot shows two main strikes and they are in N20º-30ºE and N50º-60ºW directions.

3.6.3- Third station

This station has coordinate E (x axis): 2317096 and N (y axis): 614600 and numbers are in the Lambert coordinates. Lithology at this station is limestone and Asmari-Jahrum formations are exposed. Figure 22 shows rosette plot of lineaments at third station. The rosette plot

shows there are two main strikes and are in N0º-10ºE and N60º-70ºE directions.

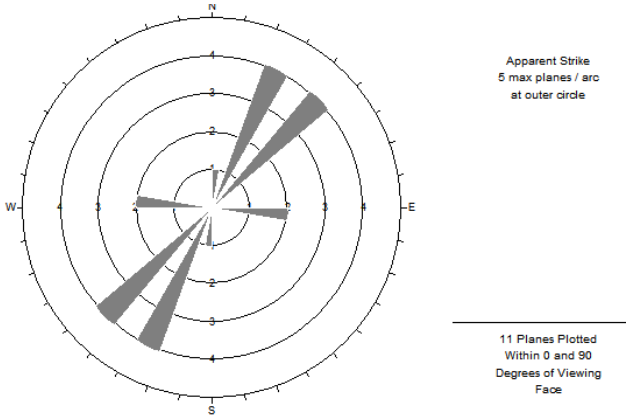

Figure 20) Rosette plot at first station.

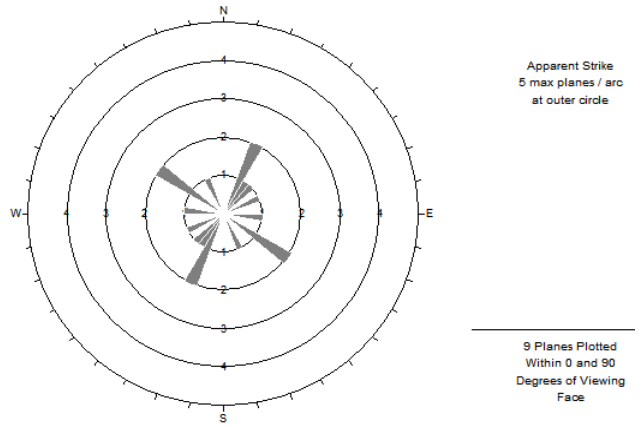

Figure 21) Rosette plot at second station.

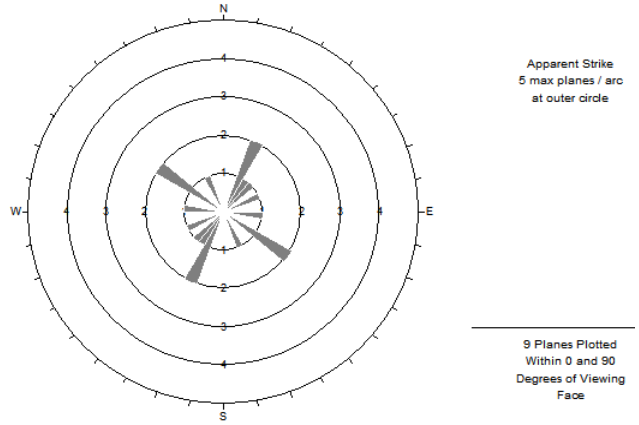

Figure 22) Rosette plot at third station.

By comparing the measured lineaments in the stations and lineaments map can see that the measured lineaments and extracted lineament from satellite image are consistent with each other. Only some of fractures were measured in the stations that are not existent in the lineaments map. This issue is related to the resolution of satellite image and because the image is not high resolution only able to identify the big fractures. Therefore, for more accurate and more detailed studies, it is required that use the satellite images with higher resolution.

4– Conclusions

Utilizing different image processing techniques has been an efficient tool for investigating lineaments in Tabnak field. 847 lineaments were effectively identified and extracted. Lineaments in different parts of the field are not similarly distributed. The northwestern part of the field, however, is characterized with higher density than the other parts. The entire field indicates lineaments strikes in different directions but the main orientation of lineaments is on NE-SW. The three dominant lineament sets with strikes are towards the N80º-90ºW, N40º-50ºE and N20º-30ºE directions.

Acknowledgments:

The author appreciates Dr. O. Cengiz and Dr. R. Chaabouni for their comments which help him to improve manuscript.

References:

Alaa, M., Katsuaki, K. 2006. Tectonic architecture through Landsat-7 ETM$^+$/SRTM DEM-derived lineaments and relationship to the hydrogeologic setting in Siwa region, NW Egypt. Journal of African Earth Sciences: 45, 467–477.

Alamashoor, S. S., Tijia, H. D. 1987. A prominent fault across the Malaysia-Thai boundary a preliminary report Warta Geologi. Newsletter of the Geological Society of Malaysia: 13, 35–37.

Blodget, H. W., Brown, G. F. 1982. Geological mapping by use of computer-enhanced imagery in western Saudi Arabia. U. S. Geological Survey Professional Paper: 1153 (Washington D. C. U. S. Printing Office). 10p.

Condid, C. D., Chavez, P. S. 1979. Basic concepts of computerized digital image processing for geologists. U. S. Geological Survey Bulletin: 1462. 16p.

Foo, K. Y. 1976. Interpretation of Landsat-1 imagery of the Third East Asia IDOE Transect across Malaysia Malaysian Geological Survey Annual Report: 1976, 183–192.

Guang, C., Xingyuan, C., Desheng, L., Xiaonian, C., Chuansheng, L., Dekun, W. 2006. The application of air and air/foam drilling technology in Tabnak gas field, southern Iran. IADC/SPE 101560, IADC/SPE Asia pacific drilling technology conference and exhibition, November 13–15, Bankok, Thailand.

Guo, G., George, S. A., Lindsey, R. P. 1996. Applications of surface lineaments and fractures for optimal horizontal well drilling and production potential estimation. SPE 37150, SPE international conference on horizontal well technology, November 18–20, Calgary, Canada.

Hobbs, W. H. 1904. Lineaments of the Atlantic border region Geological Society American Bulletin: 15, 483–506.

Juhari, M. A. 1990. Tafsiran geology imegsatelit: kajianawalmenggunakan data dari Malaysia (Geological interpretation of satellite images: preliminary study using Malaysian data). Technical Report FSFG, UKG: 4, 48–75.

Lai, K. H. 1990. The geological interpretation of a SAR image of the Upper Segama Valley, Malaysia. Asian-Pacific Remote Sensing Journal: 2, 43–45.

Napiah, A., Thach, N., Ismail, A., Mahmood, N. 1996. Geological and mineral prospecting in Kuala Kelawang area using remote sensing and GIS techniques. Proceedings of the First Malaysian Remote Sensing Society Conference on Remote Sensing and GIS. K. Lumpur 25-27 November 1996, 11–118.

Bakri Endut, N. 1993. Pemetaan lineamen (struktur) geologi kawasan Penjom, Pahang dengan menggunakan teknik penderiaan jaun. Dalam Buku Program dan Abstrak Seminar Penggunaan Data Penderiaan Jauh Dalam Sains Bumi di Kawasan Tropika Universiti Kebangsaan Malaysia, Bangi, 14-15 Disember 1993: p. 30.

Surip, N., Napiah, A., Talib, J., Ramli, K. M. N. K. 1996. Geological mapping of north east Selangor area using remoe sensing techniques Proceedings of the First Malaysian Remote Sensing Society Conference on Remote Sensing and GIS. K. Lumpur 25-27 November 1996: P1–P16.

Raj, J. K. 1982. A reappraisal of the Bok Bak fault zone Warta Geologi. Newsletter of the Geological Society of Malaysia: 8, 35–41.

Rothery, D. A. 1985. Interactive processing of satellite images for geological interpretation - a case study. Geologial Magazine: 122, 57–63.

Rowan, L. C., Wetlaufer, A. F., Goetz, A. F., Billingsley, F. C., Stewart, J. 1974. Discrimination of rock types and detection of hydrothermally altered areas in south-central Nevada by the used of computer-enhanced ERTS images. U. S. Geological Survey Professional: Paper no. 833, 35p.

Siegal, B. S., Abrams, M. J. 1976. Geological mapping using Landsat data Photogrammetric Engineering and Remote Sensing: 42, 325–337.

Sudrajat, A. 1978. Geology of southwestern Sabah on Landsat images. Sains Malaysiana: 7, 223–234.

Tija, H. D. 1971. Lineament pattern on Penang island West Malaysia. Journal of Tropical Geography: 32, 56–61.

O'leary, D. W. Friedman, J. D. ndPohn, H. A., 1976. Lineament, linear lineation some proposed new standards for old terms. Geological Society America Bulletin: 87. 1463–1469.

William, K., Overbey, J. R., Robert, L. 1968. Surface studies predict orientation of induced formation fractures in Applachian area. Presented at the spring meeting of the Eastern District, API, Division of Production, April 1968, pp. 101–105.

Received: 01 June 2014 / Accepted: 12 February 2015 / Published online: 01 March 2015

ETH Zürich Institut für Geophysik, NO H11.3, Sonneggstrasse 5, 8092 Zürich, Switzerland
E–Mail: jessica.kind@erdw.ethz.ch

Prof. David Lentz
University of New Brunswick, Department of Earth Sciences, Box 4400, 2 Bailey Drive Fredericton, NB E3B 5A3, Canada
E–Mail: dlentz@unb.ca

Dr. Anita Parbhakar–Fox
School of Earth Sciences, University of Tasmania, Private Bag 126, Hobart 7001, Australia
E–Mail: anitap1@utas.edu.au

Prof. Roberto Barbieri
Dipartimento di Scienzedella Terra e Geoambientali, Università di Bologna, Via Zamboni 67 – 40126, Bologna, Italy
E–Mail: roberto.barbieri@unibo.it

Dr. Anne–Sophie Bouvier
Faculty of Geosciences and Environment, Institut des science de la Terre, Université deLausanne, Office: 4145.4, CH–1015 Lausann, Switzerland
E–Mail: Anne–Sophie.Bouvier@unil.ch

Dr. Matthieu Angeli
The Faculty of Mathematics and Natural Sciences, Department of Geosciences, University of Oslo
Postboks 1047 Blindern, 0316 OSLO, Norway
E–Mail: matthieu.angeli@geo.uio.no

Dr. Miloš Gregor
Geological Institute of DionysStur, MlynskaDolina, Podjavorinskej 597/15 DubnicanadVahom, 01841, Slovak Republic
E–Mail: milos.gregor@hydrooffice.org

Dr. Alexander K. Stewart
Department of Geology, St. Lawrence University, Canton, NY, USA
E–mail: astewart@stlawu.edu

Dr. Cristina C. Bicalho
Environmental Geochemistry, Universidade Federal Fluminense – UFF, Niteroi–RJ, Brazil
E–mail: ccbicalho@gmail.com

Dr. Lenka Findoráková
Institute of Geotechnics, Slovak Academy of Sciences, Watsonova 45,043 53 Košice, Slovak Republic
E–Mail: findorakova@saske.sk

Dr. Mohamed Omran M. Khalifa
Geology Department, Faculty of Science, South Valley, Qena, 83523, Egypt
E–Mail: mokhalifa@svu.edu.eg

Prof. A. K. Sinha
D.Sc. (Moscow), FGS (London). B 602, VigyanVihar, Sector 56, GURGAON 122011, NCR DELHI, Haryana, India
E–Mail: anshuksinha@gmail.com